# Endoscopically Compatible MR-safe Magneto-inductive Imaging Catheter

**R.R.A. Syms[1], I.R. Young[1], M.M. Ahmad[1], S.D. Taylor-Robinson[2], M. Rea[3]**
[1]EEE Dept, Imperial College London, Exhibition Road, London, SW7 2AZ, UK
[2]Dept. of Medicine, Imperial College London, St. Mary's Hospital Campus, London, W2 1PG, UK.
[3]Dept. of Radiology, Imperial College Healthcare NHS Trust, Praed St., Paddington, London, W2 1NY, UK
r.syms@imperial.ac.uk

***Abstract*** **– Endoscopic compatibility of a catheter-based RF receiver for magnetic resonance imaging (MRI) is demonstrated. The receiver is based on a self-terminating magneto-inductive waveguide, constructed as a thin-film circuit and attached to a catheter scaffold using heat-shrink tubing. Segmentation and the use of twisted, figure-of-eight-shaped elements provide intrinsic protection against transmitter $B_1$ and E fields, respectively. $^1$H MRI and simulated magnetic resonance cholangiopancreatography are demonstrated in a 1.5 T magnetic field.**

## I. INTRODUCTION

Magnetoinductive (MI) waveguides are periodic arrangements of magnetically coupled L-C resonators [1]. Their open arrangement makes them ideally suited to couple to the RF signals inherent in magnetic resonance imaging (MRI), and MI systems have already been demonstrated to duct flux [2], provide near-field image transfer [3] and detect rotating fields [4]. A new application is internal imaging, where the natural segmentation of a MI waveguide allows intrinsic patient safety [5]. The aim of this paper is to describe a possible application for MR-safe magneto-inductive detectors in magnetic resonance imaging cholangiopancreatography (MRCP), based on a catheter receiver delivered into the biliary ductal system by a side-opening duodenoscope.

## II. PRINCIPLE

Fig. 1a shows the principle of a linear magneto-inductive RF receiver. The circuit consists of a cascade of L-C resonators, with resonant frequency $\omega_0 = 1/\surd(LC)$. For the majority of the device length, the resonators are identical, and coupled together with a constant mutual inductance $M$ to form a MI waveguide. However, at the left-hand (detector) end, the mutual inductance is $M''$ such that $\omega_0 M'' = \surd(R\omega_0 M)$. This arrangement provides matching between the waveguide (which has impedance $\omega_0 M$ at the resonant frequency) and the resistance $R$ in the detector loop. At the right-hand end, the final loop has slightly different parameters $L'$ and $C'$ such that $\omega_0 = 1/\surd(L'C')$ once again. The mutual inductance is $M'$ such that $\omega_0 M' = \surd(Z_0 \omega_0 M)$, allowing impedance matching to the input impedance $Z_0$ of the MRI scanner. Signals induced in the detector element will therefore travel as a MI wave to the input without reflection. Similarly, signals induced in the cable will generate pairs of waves, one of which will reach the detector. The circuit provides the magneto-inductive analogue of a resonant detector matched to an output transmission line. In contrast to a conventional system, it will detect MRI signals along its entire length. However, its sensitivity will clearly be highest in the resonant detector [5].

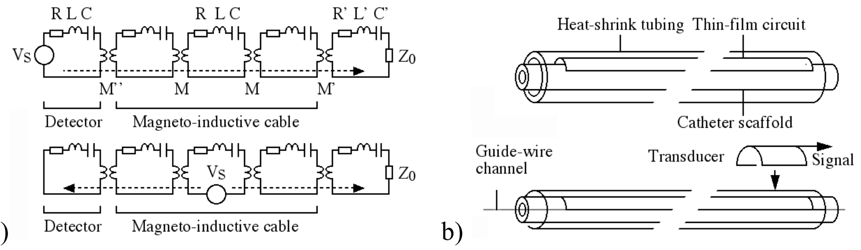

Fig. 1 a) Equivalent circuit of magneto-inductive RF receiver, and b) catheter-based implementation.

A catheter receiver based on this principle may be constructed as shown in Fig. 1b, using heat-shrink tubing to mount a thin-film circuit on a catheter scaffold and a detachable inductive transducer to provide the output connection. Suitable thin-film resonators may be constructed from copper-clad Kapton. If the inductors and capacitors are split into two-series connected elements as shown in Fig. 2a, no through vias are required, and fabrication only requires double-sided patterning. If in addition the loops are formed into figure-of-eight shapes, the circuit provides inherent decoupling from uniform $B_1$ fields, preventing perturbation to the local magnetization during the excitation phase of MRI. Finally, if the element length is less than the critical length for excitation of standing waves on an conductor immersed in tissue (27 cm at 63.8 MHz, the Larmor frequency for $^1$H MRI at 1.5 T), the circuit provides protection against heating by the strong E-fields near transmitter coil capacitors. Catheter receivers with an element length of 20 cm and an overall length of > 1.6 m have been constructed, and Fig 2b shows the different stages involved in catheter integration.

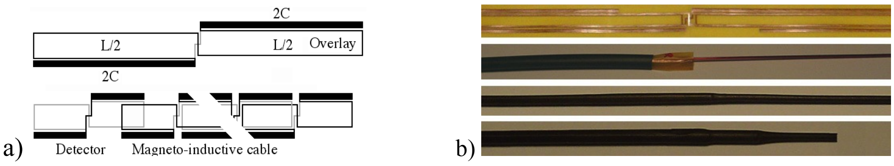

Fig. 2 a) Layout and b) construction of magneto-inductive catheter receiver.

## III. MAGNETIC RESONANCE IMAGING AND MRCP

Conventionally, the biliary and pancreatic ducts are investigated using endoscopic retrograde cholangiopancreatography (ERCP). A duodenoscope is passed down the throat to the duodenum, using a side viewing optical imaging system to locate the sphincter of Oddi (the common opening to the ducts). The instrument contains a central biopsy channel with a steerable side port, allowing cannulation with a variety of catheter tools. For example, injection of X-ray contrast agent allows imaging of the entire ductal system using X-ray fluoroscopy. However, such images only allow visualization of the duct boundaries. Catheter based RF receivers have the potential to allow high-resolution magnetic resonance cholangiopancreatography, with inherent soft tissue contrast both in and beyond the duct wall. To realize this challenging aim, a number of conditions must be satisfied. The catheter receiver must be able to pass the biopsy channel of a side-opening duodenoscope, and still operate correctly after bending through approximately 90 degrees during cannulation as shown in Fig. 3.

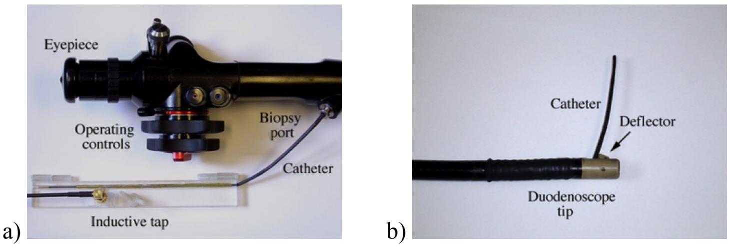

Fig. 3. Magneto-inductive catheter receiver passing MR-compatible duodenoscope: a) proximal and b) distal end.

Preliminary $^1$H magnetic resonance imaging experiments using a GE Signa Excite clinical scanner have shown that the magneto-inductive catheter receiver appears to have many of the necessary attributes. For example, Fig. 4a shows the receiver mounted on a cuboid phantom. Fig. 4b shows a coronal slice through the phantom, obtained using a spin echo sequence. The image is obtained as a multi-lobed pattern that follows the catheter track, and (as expected) is brightest at the resonant detector. Fig. 4c shows a similar image obtained with a meandered catheter track, showing that the receiver still operates correctly when bent.

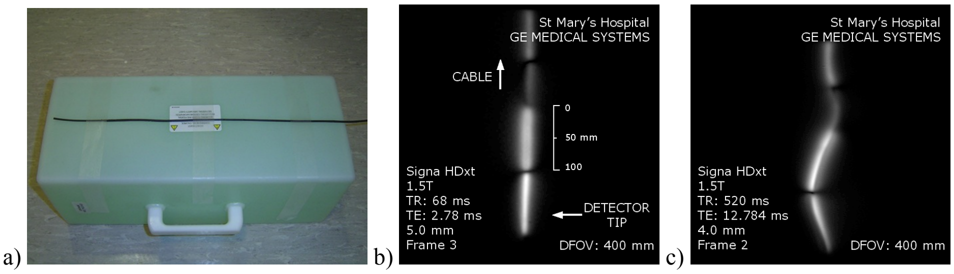

Fig. 4 $^1$H MRI: a) Cuboid phantom; b) and c) coronal images with straight and meandered catheter paths.

Fig. 5a shows a similar imaging arrangement, with an additional resolution test phantom (a cylindrical container, holding small objects immersed in signal source) mounted above the catheter. Fig. 5b shows a sagittal image of a phantom containing a M6 nut and bolt. The details of the thread are clearly resolved, suggesting the potential for high-resolution imaging. Finally, Fig. 5c shows an axial image of a phantom containing an array of small tubes with wall thickness 0.4 mm. Apart from a small artifact immediately above the catheter there is little perturbation to the magnetization, suggesting that the passive $B_1$ decoupling strategy operates correctly. High signal-to-noise ratio (SNR) is clearly obtained at some distance from the catheter.

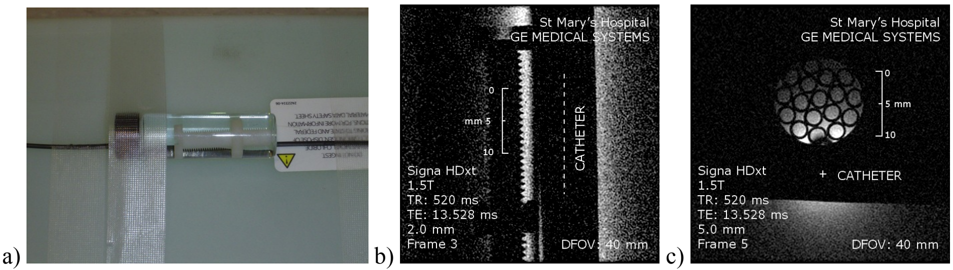

Fig. 5 $^1$H MRI: a) Resolution phantom; b) sagittal image of bolt phantom, and c) axial image of tube phantom.

Fig. 6a shows an arrangement simulating MRCP. Here the catheter receiver has been passed through a dummy duodenoscope tip immersed in signal source, and emerges at 90 degrees. Figs. 6b and 6c show sagittal images obtained using the body coil and catheter receiver respectively. In the former case, the image is uniformly bright in regions occupied by the signal source, but with a relatively poor SNR. In the latter, the field of view is localized to the immediate vicinity of the catheter. However, here a much larger (12x) SNR is obtained. Although embryonic, these results are promising for high-resolution local imaging of the biliary duct.

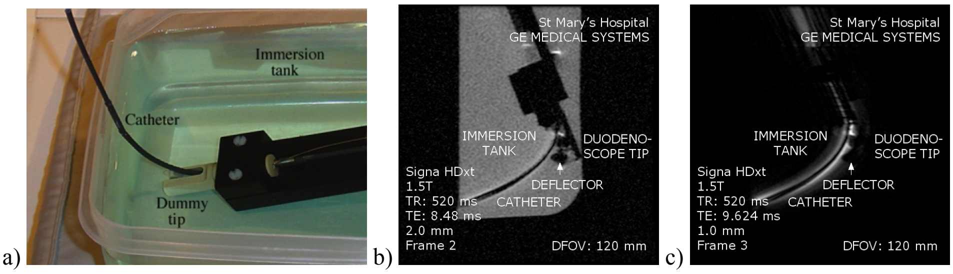

Fig. 6 Simulated MRCP: a) Arrangement, b) and c) sagittal images obtained with the body coil and catheter receiver.

## VI. CONCLUSIONS

A catheter receiver for $^1$H magnetic resonance imaging based on a linear magneto-inductive waveguide has been demonstrated at 1.5 T. Preliminary experiments have shown that the receivers can pass through the biopsy channel of a duodenoscope, provide inherent decoupling from uniform external $B_1$ fields and yield images with high signal-to-noise ratio even when bent in simulation of magnetic resonance cholangiopancreatography.

## REFERENCES

[1] E. Shamonina, V.A. Kalinin, K.H. Ringhofer and L. Solymar, "Magnetoinductive waveguide" *Elect. Lett.* vol. 38, pp. 371-373, 2002.
[2] M.C. Wiltshire, E. Shamonina, L. Solymar, I.R. Young "Development of metamaterial components for use in MRI and NMR systems" *Proc. ISMRM 11*, pp. 1582, 2004.
[3] M.J. Freire, R. Marques, L. Jelinek, "Experimental demonstration of a $\mu_r = -1$ metamaterial lens for magnetic resonance imaging" *Appl. Phys. Lett.* vol. 93, 231108, 2008.
[4] R.R.A. Syms, T. Floume, I.R. Young, L. Solymar, M. Rea, "Flexible magnetoinductive ring MRI detector: design for invariant nearest neighbour coupling" *Metamaterials* vol. 4, pp. 1-14, 2010.
[5] R.R.A. Syms, I.R. Young, M.M. Ahmad, M. Rea "Magnetic resonance imaging with linear magneto-inductive waveguides" *J. Appl. Phys.* vol. 112, 114911, 2012.